

## Research Article

# Dye-Sensitized Solar Cells Based on $\text{Bi}_4\text{Ti}_3\text{O}_{12}$

Zeng Chen, Shengjun Li, and Weifeng Zhang

Key Laboratory of Photovoltaic Materials of Henan Province and School of Physics & Electronics, Henan University, Kaifeng 475001, China

Correspondence should be addressed to Weifeng Zhang, wfzhang@henu.edu.cn

Received 10 March 2011; Revised 2 June 2011; Accepted 7 June 2011

Academic Editor: Masanori Tachiya

Copyright © 2011 Zeng Chen et al. This is an open access article distributed under the Creative Commons Attribution License, which permits unrestricted use, distribution, and reproduction in any medium, provided the original work is properly cited.

Bismuth titanate ( $\text{Bi}_4\text{Ti}_3\text{O}_{12}$ ) particles were synthesized by hydrothermal treatment and nanoporous thin films were prepared on conducting glass substrates. The structures and morphologies of the samples were examined with X-ray diffraction and scanning electron microscope (SEM). Significant absorbance spectra emerged in visible region which indicated the efficient sensitization of  $\text{Bi}_4\text{Ti}_3\text{O}_{12}$  with N3 dye. Surface photovoltaic properties of the samples were investigated by surface photovoltage. The results further indicate that N3 can extend the photovoltaic response range of  $\text{Bi}_4\text{Ti}_3\text{O}_{12}$  nanoparticles to the visible region, which shows potential application in dye-sensitized solar cell. As a working electrode in dye-sensitized solar cells (DSSCs), the overall efficiency reached 0.48% after  $\text{TiO}_2$  modification.

## 1. Introduction

Dye-sensitized solar cells (DSSCs) have attracted the attention of scientists all over the world because of their relatively high efficiency and low-cost production [1, 2]. In dye-sensitized solar cells, the most important part is the nanoporous electrode made of wideband gap semiconductor for supporting dye molecules and transporting photo-injected electrons. Previous research has been limited to simple binary oxides, including  $\text{TiO}_2$ ,  $\text{ZnO}$  [3],  $\text{SnO}_2$  [4],  $\text{Nb}_2\text{O}_5$  [5],  $\text{WO}_3$  [6], and  $\text{In}_2\text{O}_3$  [7], and so forth. Little attention has been carried out on the ternary oxides, except for  $\text{SrTiO}_3$  [8] and  $\text{Zn}_2\text{SnO}_4$  [9]. However, the multication oxides show more advantages for the tuning of materials' chemical and physical properties by altering the compositions [10, 11]. It is interesting to investigate the potential applications of new ternary oxides in DSSCs for higher photoelectric conversion efficiency.

Bismuth titanate,  $\text{Bi}_4\text{Ti}_3\text{O}_{12}$ , behaves as an n-type semiconductor with an indirect band gap of 3.2 eV [12, 13]. It is an important ceramic material widely studied on its nonvolatile memory, optical memory, piezoelectric, and photocatalytic properties [14–17]. Its photovoltaic properties, however, have scarcely been reported. In the previous work, we have investigated the surface photovoltage response of thin compact  $\text{Bi}_4\text{Ti}_3\text{O}_{12}$  film on fluorine-doped tin oxide

conductive glass substrate [13]. In this work, nanoporous  $\text{Bi}_4\text{Ti}_3\text{O}_{12}$  electrode was prepared and sensitized with N3 dye and the photoelectric properties was investigated.

## 2. Experimental

*2.1. Preparation and Characterization of Nanocrystal  $\text{Bi}_4\text{Ti}_3\text{O}_{12}$  Electrode.*  $\text{Bi}(\text{NO}_3)_3 \cdot 5\text{H}_2\text{O}$  and  $\text{Ti}(\text{OC}_4\text{H}_9)_4$  were used as the bismuth and titanium sources, respectively, for the hydrothermal synthesis of  $\text{Bi}_4\text{Ti}_3\text{O}_{12}$ . The two sources were dissolved in glacial acetic acid to form two transparent solutions. A little acetylacetone were added as stabilizer. Then, bismuth nitrate solution was slowly added to the tetrabutyl titanate solution. Eight percent excess  $\text{Bi}(\text{NO}_3)_3 \cdot 5\text{H}_2\text{O}$  was added to compensate for the Bi loss during the thermal annealing. After magnetic stirring for 24 hours, sodium carbonate ( $\text{Na}_2\text{CO}_3$ ) aqueous solution was added dropwise to the mixture under vigorous stirring to form a yellow colloid. The mixture was autoclaved at 190°C for 12 h. The resulting precipitates were ultrasonically dispersed and washed thoroughly with deionized water and ethanol successively, then dried at 60°C in an oven. The sample was sintered at 690°C for two hours to form  $\text{Bi}_4\text{Ti}_3\text{O}_{12}$ .

$\text{Bi}_4\text{Ti}_3\text{O}_{12}$  particles were suspended, mixing 0.6 g with 0.1 g of ethylcellulose in 5 mL of 1-butanol. Thin porous

$\text{Bi}_4\text{Ti}_3\text{O}_{12}$  films were prepared by spreading the suspension onto conducting glass substrates ( $30\ \Omega/\square$ ), followed by heating at  $450^\circ\text{C}$  for 30 min in air to eliminate the ethylcellulose.  $\text{TiO}_2$  coated  $\text{Bi}_4\text{Ti}_3\text{O}_{12}$  was also prepared by adding tetrabutyl titanate to the colloid of  $\text{Bi}_4\text{Ti}_3\text{O}_{12}$  in 1-butanol before the doctor blading process.

The crystalline phases of the samples were characterized by DX-2500 X-ray diffractometer (XRD) with a monochromatized  $\text{Cu K}\alpha$  irradiation ( $\lambda = 0.154145\ \text{nm}$ ). The morphologies of the samples were determined using a HitachiS-4300F field emission scanning electron microscope (SEM). The absorption spectrum was measured by a UV-vis-NIR photospectrometer (Varian Cary 5000). To investigate the charge separation behavior at the surface of the samples, the surface photovoltage spectroscopy (SPS) was carried out with a home-built apparatus including a 500 W xenon lamp (CHF XQ500 W), a double-grating monochromator (Zolix SP500), a lock-in amplifier (SR830-DSP), a light chopper (SR540), and so on [18].

**2.2. Fabrication and Characterization of Dye-Sensitized Solar Cells.** Nanoporous  $\text{Bi}_4\text{Ti}_3\text{O}_{12}$  films were dipped into the  $5 \times 10^4\ \text{mol}$  ethanol solution of *cis*-bis(thiocyanato)-*N,N'*-bis(2,2'-bipyridyl-4,4'-dicarboxylate) ruthenium (II) (N3 dye) for more than 48 h to absorb enough sensitizer. The counter electrode was Pt foil. The mixture of 0.6 M dimethylpropylimidazolium iodide, 0.1 M iodine, 0.5 M 4-*tert*butylpyridine, and 0.1 M lithium iodide in methoxy acetonitrile was selected to be the electrolyte of DSSCs. The counter electrode and the dye-sensitized  $\text{Bi}_4\text{Ti}_3\text{O}_{12}$  electrode were clamped firmly together. The redox electrolyte solution was introduced into the porous nanocrystalline  $\text{Bi}_4\text{Ti}_3\text{O}_{12}$  film by capillary action.

The photoelectrochemical characteristics of DSSCs were measured by the photocurrent-voltage curve (*I-V* curves) measurement with an Electrochemical Workstation (Shanghai Chen-hua Instrument Co, China) under the simulated solar light. A 500 W xenon lamp was used as the light source. The incident light intensity was  $100\ \text{mW}\cdot\text{cm}^{-2}$  measured by a Radiation Meter (FZ-A, Beijing Normal University, China) and the active cell area was  $0.25\ \text{cm}^2$ . The flat band potential was measured by the Mott-Schottky analysis method with the potential range from 0 to 1.0 V [19, 20].

### 3. Results and Discussion

**3.1. Structures and Morphologies.** The XRD pattern of the as-prepared  $\text{Bi}_4\text{Ti}_3\text{O}_{12}$  and  $\text{TiO}_2$  coated  $\text{Bi}_4\text{Ti}_3\text{O}_{12}$  nanoparticles is shown in Figure 1. The samples exhibit well-crystallized perovskite phase of  $\text{Bi}_4\text{Ti}_3\text{O}_{12}$  according to the JCPDS database card number 47-0398. The average particle size calculated is around 56 nm by Scherrer formula. There was no diffraction peak for  $\text{TiO}_2$  after the coating process.

Figure 2 shows the surface morphology image of the  $\text{Bi}_4\text{Ti}_3\text{O}_{12}$  film (a) and  $\text{TiO}_2$  coated  $\text{Bi}_4\text{Ti}_3\text{O}_{12}$  (b) in top views. It can be seen that the  $\text{Bi}_4\text{Ti}_3\text{O}_{12}$  film grown on FTO substrates possesses a high degree of porosity which was the key factor to obtain efficient dye-sensitized solar cells. The

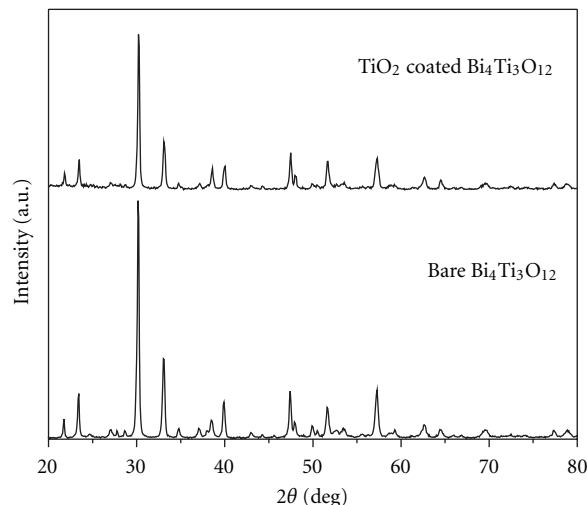


FIGURE 1: X-ray diffraction pattern of  $\text{Bi}_4\text{Ti}_3\text{O}_{12}$ - and  $\text{TiO}_2$ -coated  $\text{Bi}_4\text{Ti}_3\text{O}_{12}$  nanoparticles annealed at  $690^\circ\text{C}$  for 2 h.

size of the nanoparticles is in the range of 100–200 nm which is much larger than the XRD result. The thickness of the  $\text{Bi}_4\text{Ti}_3\text{O}_{12}$  film is about  $15\ \mu\text{m}$ . After the modification, most of the  $\text{Bi}_4\text{Ti}_3\text{O}_{12}$  nanoparticles were coated with  $\text{TiO}_2$ .

**3.2. UV-vis Absorption Spectra.** The UV-vis absorption spectra of N3 dye in ethanol solution (curve a),  $\text{Bi}_4\text{Ti}_3\text{O}_{12}$  nanoparticles (curve b), and N3-sensitized  $\text{Bi}_4\text{Ti}_3\text{O}_{12}$  nanoparticles (curve c) are illustrated in Figure 3. The spectrum (curve b) of  $\text{Bi}_4\text{Ti}_3\text{O}_{12}$  nanoparticles exhibits a typical optical absorption behavior of a wide-band gap semiconducting oxide, having an intense absorption band with a steep edge. When N3 dye molecules are adsorbed onto the surface of the  $\text{Bi}_4\text{Ti}_3\text{O}_{12}$  nanoparticles, a new absorption band around 524 nm emerges in the visible region (curve c) compared with that of bare  $\text{Bi}_4\text{Ti}_3\text{O}_{12}$  nanoparticles (curve b) which evidently originates from the absorption of dye molecules. However, the maximum absorption at 500 nm of pure N3 dye is shifted to 524 nm. The red shift might be attributed to the interaction between the dye molecules and semiconductor surface which shows the potential application in dye-sensitized solar cells [21–23].

**3.3. Surface Photovoltage Spectroscopy Analysis.** In our previous work, it has been found that the  $\text{Bi}_4\text{Ti}_3\text{O}_{12}$  thin compact film exhibited obvious surface photovoltaic response, which is attributed to the electronic transition from the O 2p valence band to the Ti 3d conduction band. Figure 4 shows the SPS spectra of bare and N3 sensitized  $\text{Bi}_4\text{Ti}_3\text{O}_{12}$  nanoparticles. The surface photovoltaic response of the bare  $\text{Bi}_4\text{Ti}_3\text{O}_{12}$  nanoparticles appeared in the wavelength range of 310–420 nm with a maximum at 361 nm. After the absorption of N3, a new SPS response band emerges in the visible region of 420–600 nm, which extends the onset of the surface photovoltaic response of  $\text{Bi}_4\text{Ti}_3\text{O}_{12}$  from 420 to 600 nm. The clear SPV peak indicates that photo-induced electron-hole pairs are easily and effectively separated on the basis of the SPS principle in the visible light.

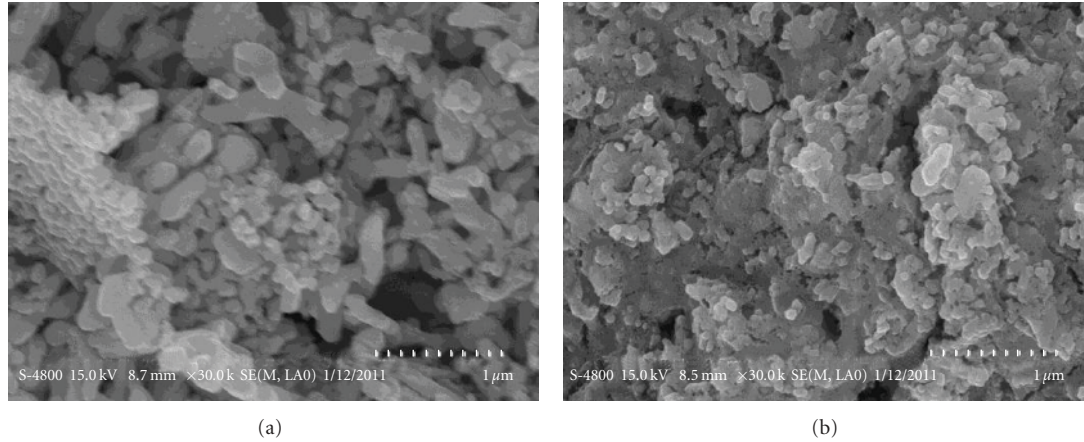


FIGURE 2: SEM micrographs the thin film. (a)  $\text{Bi}_4\text{Ti}_3\text{O}_{12}$  top view, (b)  $\text{TiO}_2$  coated  $\text{Bi}_4\text{Ti}_3\text{O}_{12}$ .

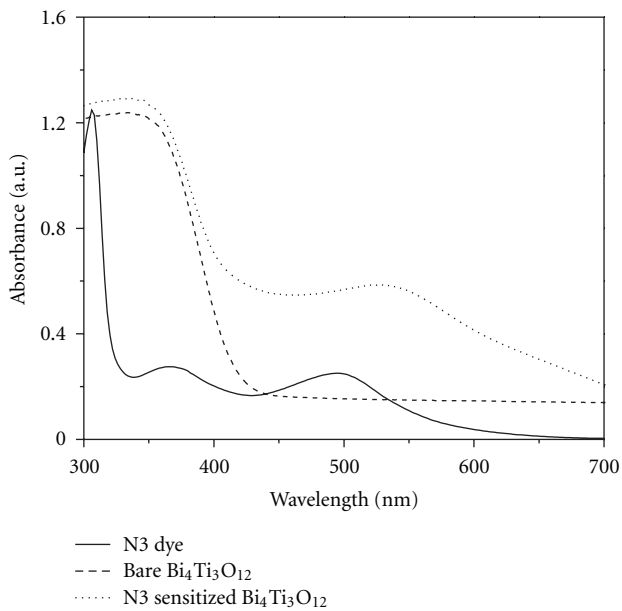


FIGURE 3: UV-vis absorption spectra of N3 (curve a),  $\text{Bi}_4\text{Ti}_3\text{O}_{12}$  nanoparticles (curve b), and N3 sensitized  $\text{Bi}_4\text{Ti}_3\text{O}_{12}$  nanoparticles (curve c).

**3.4. Performance of DSSCs.** Based on the previous study, application of  $\text{Bi}_4\text{Ti}_3\text{O}_{12}$  film in dye-sensitized solar cells seems to be possible. However, the adsorption of dye on  $\text{Bi}_4\text{Ti}_3\text{O}_{12}$  film is slow. In this study, all the photoelectrode was soaked in the dye ethanol solution at least for 48 h to achieve better dye adsorption. Figure 5 shows the  $J$ - $V$  characteristics of the DSC based on pure  $\text{Bi}_4\text{Ti}_3\text{O}_{12}$ , pure  $\text{TiO}_2$ , and  $\text{TiO}_2$ -modified  $\text{Bi}_4\text{Ti}_3\text{O}_{12}$  nanoporous electrodes. It can be seen that the photoelectrical performance of  $\text{Bi}_4\text{Ti}_3\text{O}_{12}$  is similar with the simple binary oxides, such as  $\text{TiO}_2$  and  $\text{ZnO}$ . But the overall light to electricity conversion efficiency is as low as 0.02%. The factors which contribute to the conversion efficiency are short-circuit current ( $J_{SC}$ ), open-circuit voltage ( $V_{OC}$ ), and the fill factor ( $FF$ ). The

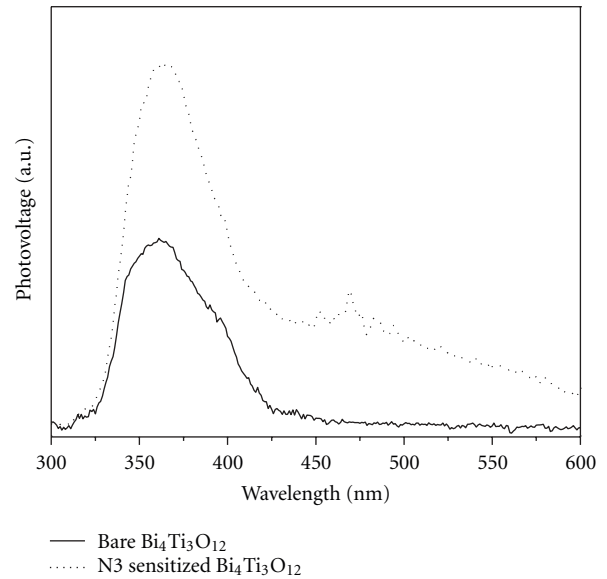


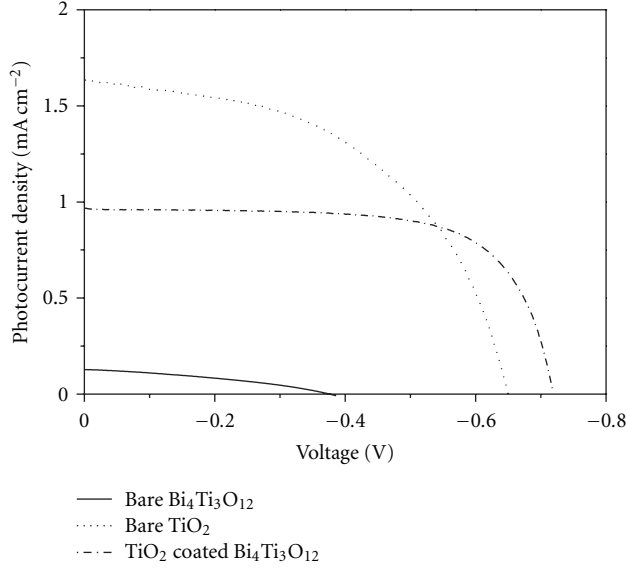
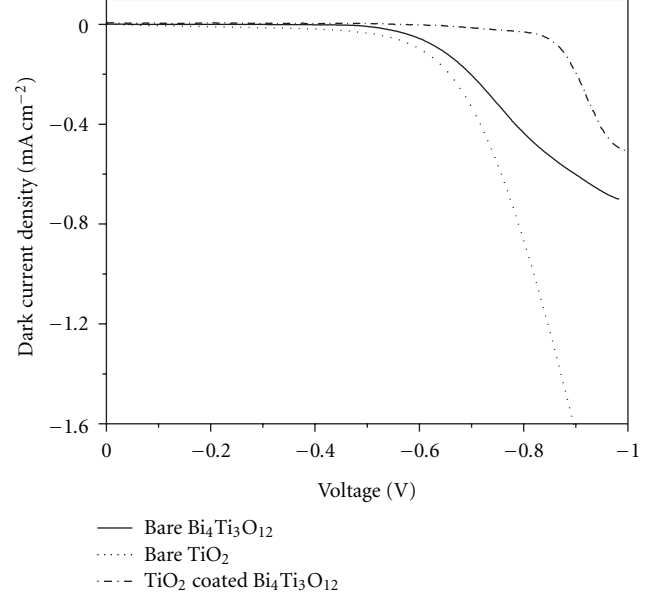
FIGURE 4: SPS spectra of  $\text{Bi}_4\text{Ti}_3\text{O}_{12}$  nanoparticles (curve a) and N3-sensitized  $\text{Bi}_4\text{Ti}_3\text{O}_{12}$  nanoparticles (curve b).

three main parameters are  $0.13 \text{ mA cm}^{-2}$ , 0.38 V, and 0.40, respectively (shown in Table 1.).

To improve the photoelectrical performance of  $\text{Bi}_4\text{Ti}_3\text{O}_{12}$  electrode, the efficient way is coating the photoelectrode with other semiconducting oxide, such as  $\text{Al}_2\text{O}_3$ ,  $\text{ZnO}$ , and so on [4, 24]. Here, we modified the  $\text{Bi}_4\text{Ti}_3\text{O}_{12}$  film with  $\text{TiO}_2$  by addition of 5% (a.t.) tetrabutyl titanate to the colloid of  $\text{Bi}_4\text{Ti}_3\text{O}_{12}$  in 1-butanol before the doctor blading process. Remarkable improvements were found in every aspect of short-circuit current ( $J_{SC}$ ), open-circuit voltage ( $V_{OC}$ ), and the fill factor ( $ff$ ) (shown in Table 1.). The  $J_{SC}$  was improved by nearly seven times. The  $V_{OC}$  and fill factor also showed an improvement of 340 mV and 0.29. The overall efficiency reached 0.48%. The Property of the pure  $\text{TiO}_2$  electrode prepared by the doctor blading of the 1-butanol solution of tetrabutyl titanate was also given in Figure 5. It can be seen that the  $\text{TiO}_2$  modified  $\text{Bi}_4\text{Ti}_3\text{O}_{12}$  also shows higher

TABLE 1: Photoelectrochemical parameters of DSSCs using bare and 5 at % TiO<sub>2</sub>-modified Bi<sub>4</sub>Ti<sub>3</sub>O<sub>12</sub> nanoporous electrodes.

Sample	$J_{SC}$ /mA cm <sup>-2</sup>	$V_{OC}$ /mV	$ff$	$\eta/\%$
Bare Bi <sub>4</sub> Ti <sub>3</sub> O <sub>12</sub> /N3	0.13	0.38	0.40	0.02
TiO <sub>2</sub> /N3	1.64	0.65	0.50	0.53
Bi <sub>4</sub> Ti <sub>3</sub> O <sub>12</sub> /TiO <sub>2</sub> /N3	0.97	0.72	0.69	0.48

FIGURE 5:  $J$ - $V$  characteristics of bare (curve a) and 5 at % TiO<sub>2</sub>-modified Bi<sub>4</sub>Ti<sub>3</sub>O<sub>12</sub> (curve b) thin films.FIGURE 6: Dark current characteristics of bare (curve a) and 5 at % TiO<sub>2</sub>-modified Bi<sub>4</sub>Ti<sub>3</sub>O<sub>12</sub> (curve b) thin films.

open circuit voltage than the pure TiO<sub>2</sub> electrode. To explore the causes for the enhancement of the photoelectrochemical properties of DSSCs, the dye absorption, flat band potential, and dark current were investigated.

The restriction of charge recombination at the semiconductor/dye/electrolyte interface is an efficient method for the improvement of  $V_{OC}$  and FF of DSSCs [25, 26]. The dark current arises from the reduction of triiodide and oxidized dye molecule by conduction band electrons of semiconductor films [25, 26]. The dark current measurement is an apparent analysis on the interface charge recombination. Figure 6 addresses the dark current for the dye-sensitized solar cells using pure Bi<sub>4</sub>Ti<sub>3</sub>O<sub>12</sub>, pure TiO<sub>2</sub>, and TiO<sub>2</sub>-modified Bi<sub>4</sub>Ti<sub>3</sub>O<sub>12</sub> nanoporous electrodes. The TiO<sub>2</sub>-modified Bi<sub>4</sub>Ti<sub>3</sub>O<sub>12</sub> shows lower recombination than pure Bi<sub>4</sub>Ti<sub>3</sub>O<sub>12</sub>, and pure TiO<sub>2</sub> which contributes to the elevation of  $V_{OC}$  and fill factor.

The flat band potential ( $V_{fb}$ ) of pure Bi<sub>4</sub>Ti<sub>3</sub>O<sub>12</sub>, pure TiO<sub>2</sub>, and TiO<sub>2</sub> coated Bi<sub>4</sub>Ti<sub>3</sub>O<sub>12</sub> electrode were evaluated through the Mott-Schottky analysis method. This analysis method is based on the capacitance versus applied potential measurement. The relationship between the capacitance and the applied potential can be expressed by the following equation:

$$\frac{1}{C_{SC}^2} = \frac{2(|V - V_{fb}| - kT/e)}{\epsilon\epsilon_0 e N_D}, \quad (1)$$

[27] where  $C_{SC}$  is the space-charge capacitance,  $\epsilon$  is the dielectric constant of the semiconductor,  $\epsilon_0$  is the permittivity of free space,  $N_D$  is the dopant density,  $V_{fb}$  is the flat band potential, and  $V$  is the applied potential. Figure 7 shows the Mott-Schottky curves of pure Bi<sub>4</sub>Ti<sub>3</sub>O<sub>12</sub>, pure TiO<sub>2</sub>, and TiO<sub>2</sub> coated Bi<sub>4</sub>Ti<sub>3</sub>O<sub>12</sub> films. The plot of  $C_{SC}^2$  versus polarization potential shows an X-intercept corresponding to  $V_{fb}$ . The flat band potential of pure Bi<sub>4</sub>Ti<sub>3</sub>O<sub>12</sub> and pure TiO<sub>2</sub> was determined to be about  $-0.58$  V and  $-0.47$  V (versus Ag/AgCl). But the  $V_{fb}$  of TiO<sub>2</sub> coated Bi<sub>4</sub>Ti<sub>3</sub>O<sub>12</sub> shifts significantly toward the cathodic potential which should cause the improvement of open-circuit voltage ( $V_{OC}$ ) [27, 28].

The amount of dye absorption is one of the important factors on the short-circuit current of DSSCs. The dye absorbed on Bi<sub>4</sub>Ti<sub>3</sub>O<sub>12</sub> electrode is about  $1.4E-8$  mol cm<sup>-2</sup> which contributes to the low photocurrent. However, no significant change was found in our study before and after TiO<sub>2</sub> coating on the Bi<sub>4</sub>Ti<sub>3</sub>O<sub>12</sub> films. So other controlling process should exist, such as the electron transfer process from excited dye molecular to the conduction band of Bi<sub>4</sub>Ti<sub>3</sub>O<sub>12</sub> and the electron transport process in the Bi<sub>4</sub>Ti<sub>3</sub>O<sub>12</sub> film. Though the overall efficiency of Bi<sub>4</sub>Ti<sub>3</sub>O<sub>12</sub> is severely lower than that of TiO<sub>2</sub>, there are many ways to ameliorate the performance for this multication oxide, the variation of the relative Bi/Ti ratio, the partial replacement of Bi or Ti



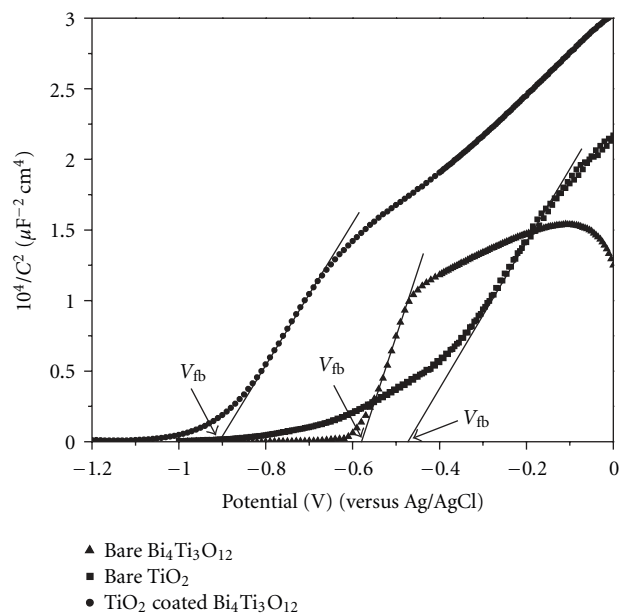


FIGURE 7: Mott-Schottky plots of bare (curve a) and 5 at %  $\text{TiO}_2$ -modified  $\text{Bi}_4\text{Ti}_3\text{O}_{12}$  (curve b) thin films,  $V_{fb}$ , the flat band potential.

by other metal ion. From this work we can conclude that  $\text{Bi}_4\text{Ti}_3\text{O}_{12}$  film is a potential photoanode material for DSSCs.

#### 4. Conclusions

In conclusion,  $\text{Bi}_4\text{Ti}_3\text{O}_{12}$  film could be efficiently sensitized with N3 dye. The sensitized  $\text{Bi}_4\text{Ti}_3\text{O}_{12}$  film shows significant absorbance and surface photovoltaic response in visible light which indicates the emergence of chemical interaction between the dye molecules and semiconductor surface. This ternary oxide exhibited similar photoelectrical performance with  $\text{TiO}_2$ . But poor performance was obtained because of the severe charge recombination and lower conduction band edge. After  $\text{TiO}_2$  modification, the three main parameters short-circuit current ( $J_{SC}$ ), open-circuit voltage ( $V_{OC}$ ), and the fill factor ( $FF$ ) are  $0.97 \text{ mA cm}^{-2}$ ,  $0.72 \text{ V}$ , and  $0.69$ , respectively. The overall efficiency reached  $0.48\%$ . Potential improvement can be anticipated by the decrease of the particle size and optimization of the compositions.

#### Acknowledgments

This work was supported by the Basic and Frontier Technology Research Programs of the Department of Science & Technology of Henan Province (no. 112300410004), the Key Technologies R & D Program of Henan Province (no. 092102210005), and the Research Fund of Henan University (no. 2010ZRZD07).

#### References

[1] B. O'Regan and M. Grätzel, "A low-cost, high-efficiency solar cell based on dye-sensitized colloidal  $\text{TiO}_2$  films," *Nature*, vol. 353, no. 6346, pp. 737–740, 1991.

[2] A. Hagfeldt, G. Boschloo, L. Sun, L. Kloo, and H. Pettersson, "Dye-sensitized solar cells," *Chemical Reviews*, vol. 110, no. 11, pp. 6595–6663, 2010.

[3] S. Rani, P. Suri, P. K. Shishodia, and R. M. Mehra, "Synthesis of nanocrystalline  $\text{ZnO}$  powder via sol-gel route for dye-sensitized solar cells," *Solar Energy Materials and Solar Cells*, vol. 92, no. 12, pp. 1639–1645, 2008.

[4] A. Kay and M. Grätzel, "Dye-sensitized core-shell nanocrystals: improved efficiency of mesoporous tin oxide electrodes coated with a thin layer of an insulating oxide," *Chemistry of Materials*, vol. 14, no. 7, pp. 2930–2935, 2002.

[5] K. Sayama, H. Sugihara, and H. Arakawa, "Photoelectrochemical properties of a porous  $\text{Nb}_2\text{O}_5$  electrode sensitized by a ruthenium dye," *Chemistry of Materials*, vol. 10, no. 12, pp. 3825–3832, 1998.

[6] H. Zheng, Y. Tachibana, and K. Kalantar-Zadeh, "Dye-sensitized solar cells based on  $\text{WO}_3$ ," *Langmuir*, vol. 26, no. 24, pp. 19148–19152, 2010.

[7] S. Mori and A. Asano, "Light intensity independent electron transport and slow charge recombination in dye-sensitized  $\text{In}_2\text{O}_3$  solar cells: in contrast to the case of  $\text{TiO}_2$ ," *Journal of Physical Chemistry C*, vol. 114, no. 30, pp. 13113–13117, 2010.

[8] S. Burnside, J. E. Moser, K. Brooks, M. Grätzel, and D. Cahen, "Nanocrystalline mesoporous strontium titanate as photoelectrode material for photosensitized solar devices: increasing photovoltage through flatband potential engineering," *Journal of Physical Chemistry B*, vol. 103, no. 43, pp. 9328–9332, 1999.

[9] B. Tan, E. Toman, Y. Li, and Y. Wu, "Zinc stannate ( $\text{Zn}_2\text{SnO}_4$ ) dye-sensitized solar cells," *Journal of the American Chemical Society*, vol. 129, no. 14, pp. 4162–4163, 2007.

[10] M. W. Chu, M. Ganne, M. T. Caldes, and L. Brohan, "X-ray photoelectron spectroscopy and high resolution electron microscopy studies of Aurivillius compounds:  $\text{Bi}_{4-x}\text{La}_x\text{Ti}_3\text{O}_{12}$  ( $x = 0, 0.5, 0.75, 1.0, 1.5, \text{ and } 2.0$ )," *Journal of Applied Physics*, vol. 91, no. 5, pp. 3178–3187, 2002.

[11] L. Wang, C. Chen, Z. Tang, C. Lu, and B. Yu, "Dependence of Zr content on electrical properties of  $\text{Bi}_{3.15}\text{Nd}_{0.85}\text{Ti}_{3-x}\text{Zr}_x\text{O}_{12}$  thin films synthesized by chemical solution deposition (CSD)," *Vacuum*, vol. 85, no. 2, pp. 203–206, 2010.

[12] L. Pintilie, I. Pintilie, and M. Alexe, "Photoconductive properties of  $\text{Bi}_4\text{Ti}_3\text{O}_{12}/\text{Si}$  heterostructures with different thickness of the  $\text{Bi}_4\text{Ti}_3\text{O}_{12}$  film," *Journal of the European Ceramic Society*, vol. 19, no. 6-7, pp. 1473–1476, 1999.

[13] W. C. Wang, H. W. Zheng, X. Y. Liu et al., "Surface photovoltage characterization of sol-gel derived  $\text{Bi}_4\text{Ti}_3\text{O}_{12}$  ferroelectric thin film on F-doped  $\text{SnO}_2$  conducting glass," *Chemical Physics Letters*, vol. 488, no. 1–3, pp. 50–53, 2010.


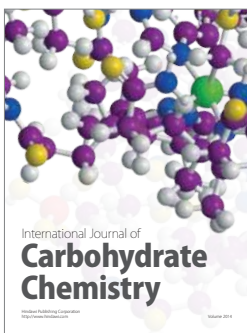
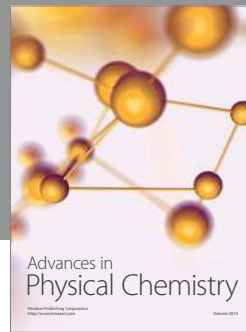
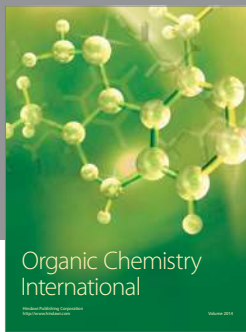
[14] J. Hou, R. V. Kumar, Y. Qu, and D. Krsmanovic, "Controlled synthesis of photoluminescent  $\text{Bi}_4\text{Ti}_3\text{O}_{12}$  nanoparticles from metal-organic polymeric precursor," *Journal of Nanoparticle Research*, vol. 12, no. 2, pp. 563–571, 2010.

[15] F. Huang, X. Lu, C. Chen et al., "Room-temperature multiferroic properties of  $\text{Bi}_{4.15}\text{Nd}_{0.85}\text{Ti}_3\text{FeO}_{15}$  thin films prepared by the metal-organic decomposition method," *Solid State Communications*, vol. 150, no. 35-36, pp. 1646–1649, 2010.

[16] A. Z. Simões, B. D. Stojanovic, M. A. Ramirez, A. A. Cavalheiro, E. Longo, and J. A. Varela, "Lanthanum-doped  $\text{Bi}_4\text{Ti}_3\text{O}_{12}$  prepared by the soft chemical method: rietveld analysis and piezoelectric properties," *Ceramics International*, vol. 34, no. 2, pp. 257–261, 2008.

[17] G. B. Kumar and S. Buddhudu, "Optical, thermal and dielectric properties of  $\text{Bi}_4(\text{TiO}_4)_3$  ceramic powders," *Ceramics International*, vol. 36, no. 6, pp. 1857–1861, 2010.

- [18] D. Cavalcoli and A. Cavallini, "Surface photovoltage spectroscopy—method and applications," *Physica Status Solidi C*, vol. 7, no. 5, pp. 1293–1300, 2010.
- [19] G. Redmond, A. O’Keeffe, C. Burgess, C. MacHale, and D. Fitzmaurice, "Spectroscopic determination of the flatband potential of transparent nanocrystalline ZnO films," *Journal of Physical Chemistry*, vol. 97, no. 42, pp. 11081–11086, 1993.
- [20] M. Wang, Q. L. Zhang, Y. X. Weng, Y. Lin, and X. R. Xiao, "Investigation of mechanisms of enhanced open-circuit photovoltage of dye-sensitized solar cells based the electrolyte containing 1-hexyl-3- methylimidazolium iodide," *Chinese Physics Letters*, vol. 23, no. 3, pp. 724–727, 2006.
- [21] P. V. Kamat, "Photochemistry on nonreactive and reactive (semiconductor) surfaces," *Chemical Reviews*, vol. 93, no. 1, pp. 267–300, 1993.
- [22] C. Bauer, G. Boschloo, E. Mukhtar, and A. Hagfeldt, "Interfacial electron-transfer dynamics in Ru(tcterpy)(NCS)<sub>3</sub>-sensitized TiO<sub>2</sub> nanocrystalline solar cells," *Journal of Physical Chemistry B*, vol. 106, no. 49, pp. 12693–12704, 2002.
- [23] Y. Zhang, H. Zhang, Y. Wang, and W. F. Zhang, "Efficient visible spectrum sensitization of BaSnO<sub>3</sub> nanoparticles with N719," *Journal of Physical Chemistry C*, vol. 112, no. 23, pp. 8553–8557, 2008.
- [24] L. Li, R. Chen, G. Jing, G. Zhang, F. Wu, and S. Chen, "Improved performance of TiO<sub>2</sub> electrodes coated with NiO by magnetron sputtering for dye-sensitized solar cells," *Applied Surface Science*, vol. 256, no. 14, pp. 4533–4537, 2010.
- [25] E. Palomares, J. N. Clifford, S. A. Haque, T. Lutz, and J. R. Durrant, "Control of charge recombination dynamics in dye sensitized solar cells by the use of conformally deposited metal oxide blocking layers," *Journal of the American Chemical Society*, vol. 125, no. 2, pp. 475–482, 2003.
- [26] J. Van De Lagemaat, N. G. Park, and A. J. Frank, "Influence of electrical potential distribution, charge transport, and recombination on the photopotential and photocurrent conversion efficiency of dye-sensitized nanocrystalline TiO<sub>2</sub> solar cells: a study by electrical impedance and optical modulation techniques," *Journal of Physical Chemistry B*, vol. 104, no. 9, pp. 2044–2052, 2000.
- [27] X. Yin, H. Zhao, L. Chen et al., "The effects of pyridine derivative additives on interface processes at nanocrystalline TiO<sub>2</sub> thin film in dye-sensitized solar cells," *Surface and Interface Analysis*, vol. 39, no. 10, pp. 809–816, 2007.
- [28] S. J. Roh, R. S. Mane, S. K. Min, W. J. Lee, C. D. Lokhande, and S. H. Han, "Achievement of 4.51% conversion efficiency using ZnO recombination barrier layer in TiO<sub>2</sub> based dye-sensitized solar cells," *Applied Physics Letters*, vol. 89, no. 25, Article ID 253512, 2006.



**Hindawi**

Submit your manuscripts at  
<http://www.hindawi.com>

